



Evaluation of a combined drought indicator against crop yield estimations and simulations over the Argentine Humid Pampas

Spennemann Pablo C.^{1,2} · Gustavo Naumann³ · Mercedes Peretti⁴ · Carmelo Cammalleri⁵ · Mercedes Salvia⁶ · Alessio Bocco⁷ · Maria Elena Fernández Long⁴ · Martin D. Maas¹ · Hyunglok Kim⁸ · Manh-Hung Le^{9,10} · John D. Bolten⁹ · Andrea Toreti¹¹ · Venkataraman Lakshmi¹²

Received: 4 April 2024 / Accepted: 16 June 2024 / Published online: 29 June 2024
© The Author(s), under exclusive licence to Springer-Verlag GmbH Austria, part of Springer Nature 2024

Abstract

Droughts pose serious threats to the agricultural sector, especially in rainfed-dominated agricultural regions like those in Argentina's Humid Pampas. This region was recently impacted by slow-evolving and long-lasting droughts as well as by flash droughts, resulting in losses reaching thousands of millions of US dollars. Improvements of drought early warning systems are essential, particularly given the projected increase in drought frequency and severity over southern South America. The spatial and temporal relationship between precipitation deficits, soil moisture and vegetation health anomalies are crucial for better understanding and representation of the agricultural droughts and their impacts. In this context, the Combined Drought Indicator (CDI) considers the causal and time-lagged relationship of these three variables. The study's objective is twofold: (1) Analyze the time-lagged response between precipitation deficits, soil moisture and satellite fAPAR anomalies; and (2) Evaluate the CDI's capability to characterize the severity of drought events on the Humid Pampas against agricultural yield estimations and simulations, as well as agricultural emergency declarations. The correlation among the variables shows strong spatial variability. The highest Pearson correlation values ($r > 0.42$) are observed over parts of the Humid Pampas for time lags of 0, 10, and 20 days between the variables. Although the CDI has limitations, such as its coarse spatial resolution and monthly temporal resolution of precipitation data, it effectively tracks the progression of major drought events in the region. The CDI's performance aligns well with estimations and simulations of soybean and corn yields, as well as official declarations of agricultural emergencies. Insights from this study also provide a basis for discussing potential improvements to the CDI. This study highlights the global and regional significance of evaluating and enhancing the CDI for effective drought monitoring, emphasizing the role of collaborative efforts for future advancements in drought early warning systems.

✉ Spennemann Pablo C.
psennemann@smn.gob.ar

¹ Present address: Consejo Nacional de Investigaciones Científicas y Técnicas (CONICET) - Servicio Meteorológico Nacional (SMN), Av. Dorrego 4019, Ciudad de Buenos Aires, República C1425GBE, Argentina

² Present address: Universidad Nacional de Tres de Febrero (UNTREF), Buenos Aires, República, Argentina

³ European Research Executive Agency, Brussels, Belgium

⁴ Facultad de Agronomía, Departamento de Recursos Naturales y Ambiente, Cátedra de Climatología y Fenología Agrícolas, Universidad de Buenos Aires, Buenos Aires, Argentina

⁵ Dipartimento di Ingegneria Civile e Ambientale (DICA), Politecnico di Milano, Milan, Italy

⁶ Grupo de Teledetección Cuantitativa, Instituto de Astronomía y Física del Espacio (IAFE, UBA/CONICET), Ciudad Autónoma de Buenos Aires, Argentina

⁷ Consultant of the Centro Regional del Clima para el Sur de Sudamérica, Buenos Aires, Argentina

⁸ School of Earth Sciences and Environmental Engineering, Gwangju Institute of Science and Technology, Gwangju, Republic of Korea

⁹ Hydrological Sciences Laboratory, NASA Goddard Space Flight Center, Greenbelt, MD, USA

¹⁰ Science Applications International Corporation, Greenbelt, MD, USA

¹¹ European Commission, Joint Research Centre (JRC), Ispra, Italy

¹² Department of Engineering Systems and Environment, University of Virginia, Charlottesville, VA, USA

1 Introduction

Droughts can impact the agricultural sector, causing major socio-economic repercussions over different regions around the globe (e.g. Kim et al. 2019). As one of the climate disasters with the most extensive global impact, droughts have affected around 1.4 billion between 2000 and 2020 (Donatti et al. 2024). These impacts can be exacerbated when the agricultural activities are carried out under rainfed conditions, as in the Humid Pampas of Argentina. This region has been recently affected by both slow evolving and long lasting droughts (2008–2009, 2011–2012 and 2020–2023, Naumann et al. 2021, 2023), as well as by fast developing droughts commonly referred to as flash droughts (Otkin et al. 2018). The combined 2008–2009 and 2011–2012 events generated losses of nearly USD 8000 M related to just the soybean production (Thomasz et al. 2019). The 2017–2018 flash drought that took place during the austral summer also caused considerable economic impacts of nearly USD 1500 M, related to corn and soybean yield reductions (Kucheruk et al. 2024; GAR, 2021). Several institutions and organizations, such as the SISSA project of the Centro Regional del Clima para el sur de América del Sur (CRC-SAS), as part of the World Meteorological Organization region III, the European and Global Drought Observatory (EDO/GDO) of the European Commission, and the United States Drought Monitor (USDMD, Svoboda et al. 2002) seek to reduce vulnerability to droughts by improving early warning systems. This goal acquires even more relevance for Argentina, as an increase in the frequency and severity of droughts under warming climate projected scenarios is expected in the region (e.g. Spinoni et al. 2020; GAR, 2021).

The characteristics and impacts of droughts depend on multiple factors, such as climate variability, vegetation types, and human activities (e.g., GAR, 2021; Hendrawan et al. 2022; Rossi et al. 2023; Thi et al. 2023). Therefore, the importance of properly characterizing the different temporal scales and regional features of droughts, requires the use of several indices and indicators as mentioned in WMO and GWP (2016). Cammalleri et al. (2021) discuss three main approaches for drought monitoring systems based on: (1) Several indices (e.g. Standardized Precipitation Index SPI, McKee et al. 1993; Standardized Precipitation Evapotranspiration, Vicente-Serrano et al. 2010) as in the Drought Information System for South America (SISSA, for its Spanish acronyms); (2) Single indices that are a combination of several indices (e.g. Soil Moisture Agricultural Drought Index SMADI, Sánchez et al. 2016); (3) Hybrid or composite indicators/indices. This last approach is used, for example by the USDMD and by the EDO/GDO systems. In particular, the USDMD uses several indices based on stream

flow, precipitation and soil moisture (Svoboda et al. 2002) from observational data and land surface models, that are then blended together assigning different weights to each index depending on the temporal scale of interest, as each index is meant to represent different drought types (e.g. meteorological, agricultural). Then, based on the spatial superposition of the different indices a drought category is assigned depending on the estimated severity. The EDO and GDO systems, instead, use the Combined Drought Indicator (CDI), developed by Sepulcre-Canto et al. (2012) and updated by Cammalleri et al. (2021).

The CDI uses a nested approach, considering the causal temporal relationship between precipitation deficits and subsequent negative anomalies in soil moisture and vegetation. In other words, this relationship is based on the fact that a precipitation shortage will lead to an eventual soil moisture deficit, which in turn could affect water availability for vegetation. As such, it seeks to represent the propagation of the water deficit signal across the terrestrial branch of the hydrological cycle and its potential impacts on vegetation and crop production/health, focusing on agricultural droughts. Sepulcre-Canto et al. (2012) analyzed the different temporal responses between the 3-month accumulated SPI (SPI-3), soil moisture simulations and fraction of Absorbed Photosynthetically Active Radiation (fAPAR) anomalies. The best agreement, over 12 meteorological stations across Europe, was found with lags of 10 and 20 days (1 and 2 dekads) between these variables. The authors concluded that this first version of CDI was able to represent the major drought events, identifying areas under agricultural drought which were coherent with observed yield reductions and emergency declarations. Cammalleri et al. (2021) proposed a new version of the CDI (v2). The authors focused on improving the temporal consistency of the CDI over Europe, throughout the evolution of long lasting drought events, by decreasing the cases showing temporal shiftings between categories from drought to no-drought conditions. In this regard, the CDI-v2 demonstrated a superior performance compared to its predecessor by effectively capturing the spatiotemporal manifestation of droughts and their resulting impacts on yield reductions. Additionally, a more coherent sequence of the category stages was observed, representing an improvement over the previous version of CDI.

The representativeness of the variables within the CDI over southern South America and the Humid Pampas, and the drought signal propagation through the terrestrial branch of the hydrological cycle are key aspects to better understanding the different time response between precipitation deficits, soil moisture and vegetation health anomalies. In this sense, a recent study by Rossi et al. (2023) highlighted that, depending on the varying characteristics of climate, vegetation, and other factors across three Brazilian

biomes, the temporal drought propagation signal can vary significantly.

Assessing the direct and indirect impacts of drought poses great challenges, differing from other meteorological hazards (e.g. floods) due to its multifaceted temporal and spatial scales, as well as its cross-sectoral and cascading effects (GAR, 2021). This study focuses solely on the direct impact of drought on the agricultural sector, examining crop yields and agricultural emergency declarations, consistent with the approach in Sepulcre-Canto et al. (2012). Furthermore, a complementary method for estimating agricultural drought impacts involves leveraging crop models to simulate yields in specific locations. Simulating the crop phenology cycle under various soil and climate conditions offers the key advantage of isolating and assessing the climatic impact on yield variations, thereby eliminating other adverse effects on crops, such as pests. However, it is essential to consider local management practices and soil characteristics to enhance model representativity. In this sense, Aramburu Merlos et al. (2015) utilizing the DSSAT model with local soil information and farming practices, documented a good representation of corn and soybean yield simulations in the Humid Pampas region. Therefore, these datasets can be used as a reference to evaluate the performance of drought indices, as drought severity should be negatively correlated with crop yield anomalies in regions affected by droughts in predominantly rainfed agricultural regions (e.g. GAR, 2021; Kim et al. 2019).

The objective of this study is twofold: (1) Analyze the lagged relationship between precipitation deficits, soil moisture and satellite-based fAPAR anomalies over southern South America and the Humid Pampas region, to detect similarities and differences with the regions where the CDI was originally developed; and (2) Evaluate the CDI (version 2, Cammalleri et al. 2021) operational configuration performance in characterizing the severity and evolution of drought events on the Humid Pampas in terms of crop yield estimations and simulations, and agricultural emergency declarations.

2 Data and methodology

2.1 Study region

This study focuses on two spatial domains: the first one corresponds to the CRC-SAS region, i.e. the area in South America south of 10°S (see Fig. 1); the second one, a subset of the first, corresponding to the Argentinian Humid Pampas (65°W 56°W and 42°S 22°S). The latter region is one of the major global breadbaskets (GAR, 2021).

2.2 Data

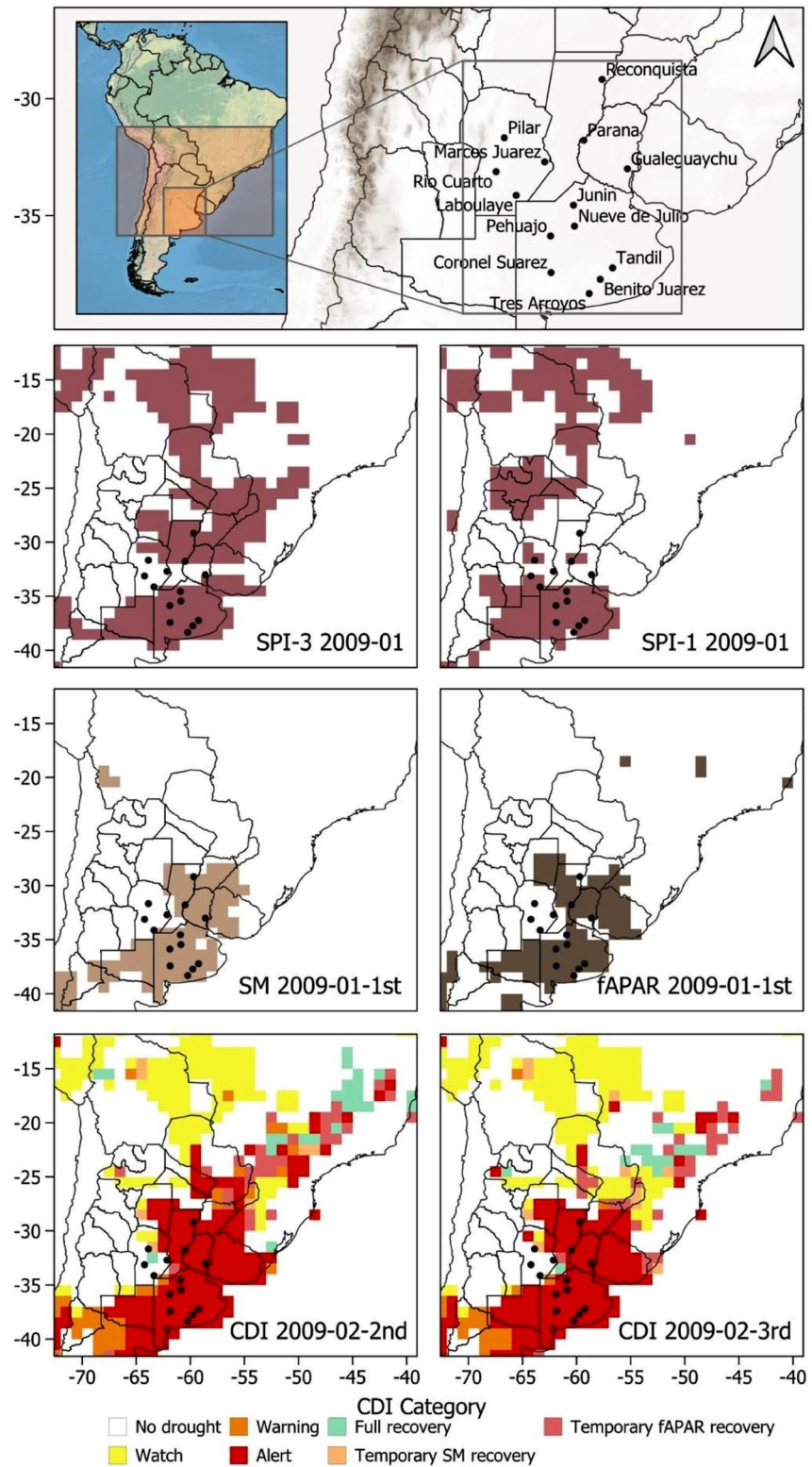
The dataset used for the CDI-v2 (hereafter CDI) computation is based on the operational Copernicus Global Drought Observatory (GDO, <https://edo.jrc.ec.europa.eu/gdo/php/index.php?id=2001>) data. Precipitation, soil moisture datasets and vegetation index are summarized in Table S1 and briefly described below. The Global Precipitation Climatology Centre (GPCC, Schamm et al. 2014) dataset is a combination of gauge station and satellite estimations, and it is used in GDO to construct the monthly SPI over different accumulation periods (e.g. SPI-1 and SPI-3). The GPCC monthly precipitation was validated over Argentina (e.g. Spennemann et al. 2015) and showed a good representation compared to ground station observations from the Argentinian National Weather Service (SMN, for its Spanish acronym).

The soil moisture ensemble product, used in the operational CDI, is based on the Triple Collocation (TP) methodology (Gruber et al. 2016; Kim et al. 2023). The TP approach uses three independent soil moisture anomaly sources, as described in Cammalleri et al. (2017), to estimate the average relative error of each one of them compared to the unknown truth. Then a weighted average is computed, with weights for each pixel that are assigned proportionally to the inverse of the local relative errors. The three independent data are anomalies of: (1) Satellite Land Surface Temperature (LST) from MODIS (Wan et al. 2002), (2) Microwave satellite surface soil moisture (0–5 cm) combined active/passive estimations from ESA-CCI (Gruber et al. 2019; Dorigo et al. 2017), and (3) LISFLOOD (De Roo et al. 2000) root zone soil moisture simulations. The anomalies for each product are calculated for each 10 day period, using a 30 day moving window, using a common climatological period (2001–2017). Subsequently, the three product anomalies are merged through the TP methodology as mentioned above. Both, LISFLOOD simulations and ESA-CCI estimations were evaluated over the Humid Pampas against in situ soil moisture observations, showing to be able to accurately represent the observed dry and wet events (Spennemann et al. 2020).

The fAPAR anomalies from MODIS are used as a vegetation biomass indicator. They are calculated for each 10 day period, after removing the corresponding 10 day mean value and dividing by the standard deviation (i.e. standardized anomalies), based on the 2001–2021 period. This index has shown to be reliable for detecting droughts and their impacts on vegetation (e.g. Gobron et al. 2005; Cammalleri et al. 2021; Peng et al. 2019).

In order to generate the operational CDI, the soil moisture and fAPAR datasets were spatially resampled, with a bilinear method, to a common and coarser resolution of

Fig. 1 Regions of interest and location of the 14 meteorological stations are shown in the upper panel, the second row shows the SPI-3 for January 2009 and the SPI-1 for January 2009, the third row shows the soil moisture anomaly (SM) for the 1st dekad of February and the fAPAR anomalies for the 2nd dekad of February, the fourth row shows the CDI for the 2nd dekad of February and the CDI for the 3rd dekad of February 2009. All variables are shown below -1 threshold, except for SPI-1 which is below -2 , and were interpolated to the $1^\circ \times 1^\circ$ GPCC precipitation spatial resolution



1°x1° corresponding to the GPCC spatial grid. In this study the period analyzed spans from 2001 to 2022.

2.3 Combined drought indicator

The CDI consists of 6 categories: WATCH, WARNING, ALERT, TEMPORARY SOIL MOISTURE RECOVERY, TEMPORARY VEGETATION (fAPAR) RECOVERY and FULL RECOVERY. As shown in Table 1, the WATCH category represents a precipitation deficit and corresponds to a SPI-3 ≤ -1 or SPI-1 ≤ -2; the WARNING category corresponds to a WATCH category + SM anomaly ≤ -1; meanwhile, the ALERT category implies a SPI-3 ≤ -1 or SPI-1 ≤ -2 and fAPAR anomalies ≤ -1.

This definition, which is the same introduced by Sepulcre-Canto et al. (2012), was expanded in Cammalleri et al. (2021) to account for the CDI category in the previous time step in order to determine how the drought conditions are evolving (e.g. recovering to non-drought conditions). In addition, to improve the temporal consistency of the drought assessment, temporary classes are added to handle short periods during which an indicator falls below the given drought threshold. For instance, the TEMPORARY SOIL MOISTURE RECOVERY category is defined when soil moisture anomalies are between 0 and -1 and with a previous CDI under a drought category (e.g. WATCH or WARNING). The TEMPORARY VEGETATION RECOVERY is defined similarly as the TEMPORARY SOIL MOISTURE RECOVERY. Meanwhile FULL RECOVERY category corresponds to the condition over all variables/indices being above the -1 threshold. A complete description of the different combinations between the variables/indices and the previous CDI category can be found in Fig. 1 of Cammalleri et al. (2021) and the related text. To give an example on how the CDI corresponding to the 3rd dekad of February 2009 is composed, in its operational configuration, Fig. 1 shows the spatial distribution of SPI-1 (January, 2009) and SPI-3 (November-January, 2008–2009), soil moisture and fAPAR anomalies for the 2nd (second) and 3rd (third) 10 day-period of February 2009 respectively, and previous CDI category (2nd dekad of February). It follows from Fig. 1, that in the region of eastern Argentina and Uruguay the red values

correspond to the ALERT category, which is related to SPI-3 and fAPAR anomalies below -1. In this example, it is clear how the drought signal already moved from a precipitation deficit to below normal soil moisture and vegetation stress conditions. In addition, the 14 meteorological stations where crop simulation were performed (see Sect. 2.3) are also shown in Fig. 1. To complement Fig. 1, Figure S1 shows the temporal evolution of the different variables and the resulting CDI category for the 2008–2009 drought event at Rio Cuarto station in central Argentina, illustrating how the CDI works.

The CDI is designed to reproduce the cascading effect of drought from precipitation to soil moisture and vegetation, exploiting regularly updated soil moisture and fAPAR data with dekad (10 day interval) frequency, and monthly SPI-3 and SPI-1. In order to evaluate the delay in response in dekadal soil moisture and fAPAR anomalies to monthly SPIs, a simultaneous and lagged Pearson correlation was carried out as in Sepulcre-Canto et al. (2012): SPI of a specific month is compared with the anomalies of soil moisture and fAPAR of the 2nd and 3rd dekad of that month (lags -1d and 0 respectively) and with the 1st, 2nd and 3rd dekads of the following month (lags +1d, +2d and +3d respectively). This was performed for the austral warm months (September-March, from 2001 to mid-2022). Only warm months were analyzed since the fAPAR better represents the crop phenology during this period (Sepulcre-Canto et al. 2012) and summer crop yields are used in the subsequent evaluations. The time period under analysis (2001–2022) is restricted by the satellite data availability.

2.4 Crop estimations and simulations, and agricultural emergency declarations

Yearly corn and soybean yield estimations from the Secretaría de Agricultura, Ganadería y Pesca (SAGyP 2022) over the 2001/02-2021/22 summer crop campaigns were used. The crop yield estimates correspond to a department spatial scale (second level administrative divisions), which include each of the 14 locations shown in Fig. 1 and listed in Table S2. In addition, the widely-used DSSAT v4.5 model suite (Hoogenboom et al. 2010) was employed to simulate corn and soybean yields based on meteorological observations, crop characteristics, and soil properties. Daily values of meteorological parameters, such as solar radiation, minimum and maximum temperatures, and precipitation from Argentina’s National Weather Service (SMN by its Spanish acronym) were used to perform the simulations. Soil data were retrieved from the Soil Atlas of Argentina, produced by the National Institute of Agricultural Research (INTA by its Spanish acronym). Dominant soils were selected for each location, and their physical and chemical properties

Table 1 The CDI (v2) threshold combination of SPI-1 and SPI-3, soil moisture (SM) and fAPAR anomalies that define the drought categories

CDI category	No Drought	WATCH	WARNING	ALERT
SPI	SPI-1 > -1 and SPI-3 > -1	SPI-1 < -1 and or SPI-3 < -1	SPI-1 < -1 and or SPI-3 < -1	SPI-1 < -1 and or SPI-3 < -1
SM Anom	> -1	> -1	≤ -1	≤ -1 or > -1
fAPAR Anom	> -1	> -1	> -1	≤ -1

were used. The predominant soils in the study area are deep mollisols with high physical and chemical fertility. Simulations were initiated with three varying soil moisture contents (20%, 50% and 100% of the field capacity), and it was assumed that biotic factors such as pests or weeds were controlled by the farmer. Consequently, yield variations are attributed solely to climate variability in each growing season. Management practices were agreed upon with experts for each simulated location, and crop coefficients were calibrated and validated using field experiments in Argentina based on previous studies (Aramburu Merlos et al. 2015; Monzon et al. 2012; Mercau et al. 2007) and personal communications with members of the Regional Agricultural Experimentation Consortium (CREA, <https://www.crea.org.ar>). In summary, each simulation consists of an ensemble between 90 and 200 members for corn and soybean yields, based on 3 different soil moisture initial conditions, varying number of sowing dates according to the location, and 3 typical soils for each location.

Crop yields were complemented by agricultural emergency declarations data from the SAGyP, which also corresponds to the department spatial scale. The agricultural emergency declarations are the primary governmental response to droughts and other natural hazards affecting the agricultural sector, and they are issued by the National System for the Prevention and Mitigation of Agricultural Emergencies and Disasters to specific regions and timeframes (GAR, 2021).

It is important to specify the difference in the spatial scale of crop estimations and simulations, as the DSSAT simulations represent a specific idealized location whereas the SAGyP estimates correspond to a spatial area that ranges from 2,253 km² to 18,394 km² over the 14 departments.

3 Results

To determine the simultaneous and lagged linear relationship between the monthly SPI-1 and SPI-3, dekadal soil moisture and fAPAR anomalies, the Pearson correlation was calculated. The correlation coefficients were calculated for different time lags for the warm months as considered in this study (September to March), and are shown in Fig. 2. The findings affirm the anticipated positive correlation among SPI, soil moisture, and fAPAR anomalies. However, the strength of this relationship varies by region and is influenced by the temporal lag between these variables. The highest and positive values were observed in Central Argentina (i.e. Humid Pampas), Uruguay, and the Northeastern part of the La Plata Basin located in Brazil. In particular, SPI-1 and soil moisture anomalies showed the highest positive correlations at lag of +1 dekad (i.e. SPI-1 of month M,

soil moisture from month M+1 and 1st dekad; more detail in Table S3), with a spatial median of $r=0.46$, encompassing the whole domain. For the -1d and 0 lags, the SPI-3 relationship with soil moisture (i.e. SPI-3 of month M, soil moisture from month M and 2nd and 3rd dekad) shows higher values compared to SPI-1- soil moisture. But, for lag+1d, +2d, and +3d, both SPI showed similar correlation values with soil moisture. Over the Humid Pampas, the correlation between SPI-3 and fAPAR was positive and higher than the correlation between SPI-1-fAPAR, specifically for the first two time lags (-1d and 0 lag). For lags +2d and +3d, both SPI accumulations showed high positive correlation values with fAPAR. The correlations between soil moisture and fAPAR showed the highest positive values for lag+2d, particularly in central and central-north Argentina, including the Humid Pampas region with a median value of $r=0.28$. It is worth noting that over the Humid Pampas there was an overall good agreement, except for SPI-1 and fAPAR (lag -1d and 0), between the different variables and time lags with significant correlation values above $r=0.40$.

The same approach described earlier was adopted to calculate correlations across the 14 selected locations within the Humid Pampas (see Fig. 1 and Table S2). Table S3 shows the median, maximum and minimum correlation of the 14 sites. Notably, the median correlation between SPI-3 and soil moisture anomalies surpasses the correlations depicted in Fig. 2, indicating also variations in the time lags that maximize the relationship between these variables. SPI-3 and soil moisture exhibited the highest median value ($r=0.64$) at lag 0, closely followed by lag -1d, lag +1d, and lag +2d, which based on a bootstrap test and a 95% confidence interval (95CI, see supplementary section) do not showed significant differences. The highest correlation was shown at lag+1d ($r=0.72$), while among the minimum correlation values, lag 0 exhibits the highest value over the 14 sites. Similarly, the median correlation between soil moisture and fAPAR anomalies peaks at lag 0 and +1d ($r=0.54$), with no significant differences for lag -1d and lag+2d (95CI). The correlation between SPI-3 and fAPAR showed the highest correlation at lag+2d. It is interesting to note that all time lags showed correlation values that are not significantly different (95CI). The maximum correlation for SPI-1 and soil moisture anomalies was observed for lag+1d with similar values for lag 0 and +2d (95CI). Lag+1d also coincides with both the highest maximum and highest minimum correlation values. Regarding SPI-1 and fAPAR anomalies, the highest correlation occurred at lag+2d, showing no statistical differences compared to lag+1d and lag+3d, with the maximum and highest minimum for the same lag+2d. A significant difference arose in the correlations between SPI-1 and SPI-3 with fAPAR, particularly at time lags of -1d and 0. Specifically, when comparing the correlations

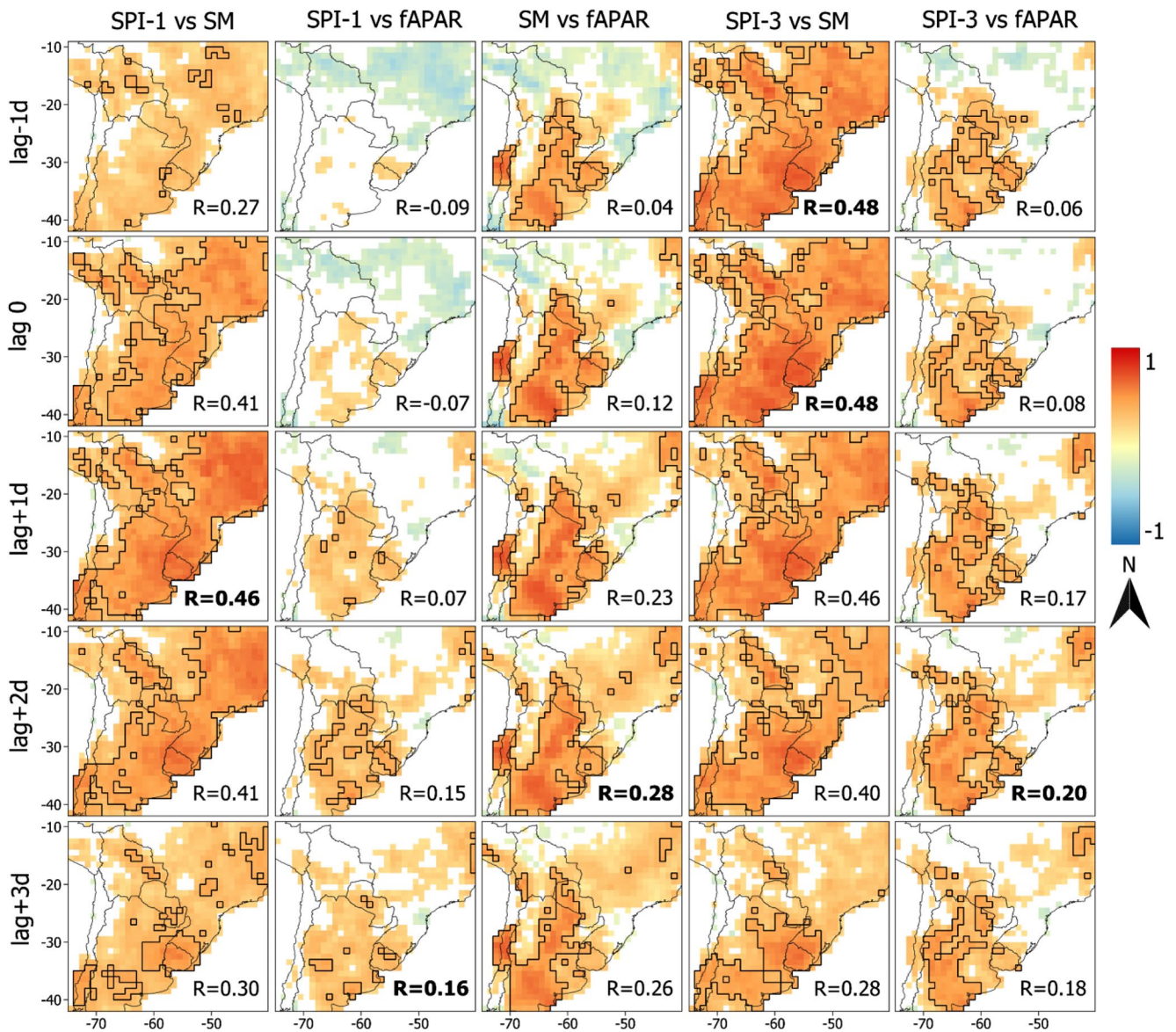


Fig. 2 Pearson correlations between the different variables and temporal lags represented by dekads (d, i.e. +1d=10 day period). Black contour represents the $r=0.40$ value and points with no significant correlation values were masked out ($p < 0.05$). Warm months September to March for 2001-mid 2022 period. Sample size for correlations with

SPI was $n=150$, and between soil moisture and fAPAR was $n=450$. The median spatial correlation is shown in the lower right corner of each panel, where the **bold** represents the highest correlation for each column

$r(\text{SPI-1}, \text{fAPAR})=-0.01$ and $r(\text{SPI-3}, \text{fAPAR})=0.33$ for lag-1d. In summary, the highest median correlations were observed between SPI-3 and soil moisture anomalies, while the lowest were found for the first temporal lags of SPI-1 and SPI-3 with fAPAR anomalies.

Figure 3 illustrates the temporal evolution of different drought categories in CDI across the 14 sites. The configuration used for CDI is derived from its operational formulation shown in Table S4. The bottom panel is accompanied by emergency declarations from SAGyP for each of the departments containing the 14 sites. This figure allows for

a qualitative analysis, comparing the more severe CDI categories with agricultural emergency declarations. In general, there was a good agreement between periods marked by WARNING and ALERT categories and the periods coinciding with emergency declarations (e.g. 2008–2009). The temporal evolution of CDI reveals certain years when severe drought events (characterized by a higher number of ALERT categories) affected only northern sites within the Pampas domain (2011, 2012, and 2013) while in other years, droughts affected mostly southern sites (2006 and 2007). Noteworthy is the 2008–2009 event, well represented by the high number of ALERT categories per dekad coinciding

Fig. 3 Heat map of the CDI (version 2) drought categories (WATCH, WARNING and ALERT) temporal evolution over the 14 locations (ordered from north to south) for the 2001–2022 period (upper panel). Heat map of periods where agricultural emergencies were issued (SAGyP, lower panel). The rectangles denote the 2008–2009 and 2017–2018 drought events



with emergency declarations across all sites. In some fast-evolving events (e.g. 2017–2018), the natural and expected progression of the drought classes was not observed over some sites, as the event reached directly the WARNING or even ALERT class. The 2017–2018 event also showed a significant percentage of sites reporting agricultural emergencies (64%).

To further analyze the impacts on agricultural yields, complementing the analysis of agricultural emergency declarations, Fig. 4 displays standardized anomalies for

departmental corn and soybean yield estimates, alongside point-based simulations for each site. The simulations are represented by the ensemble median for each site. In general, there was a good agreement between WARNING and ALERT categories in CDI and negative anomalies in corn and soybean yields in different sites. This pattern is evident not just during the 2008–2009 and 2017–2018 events, where a clear alignment is observed between drought categories and the estimated negative yield anomalies, but also across most northern stations (Pilar, Marcos Juárez, Río Cuarto,

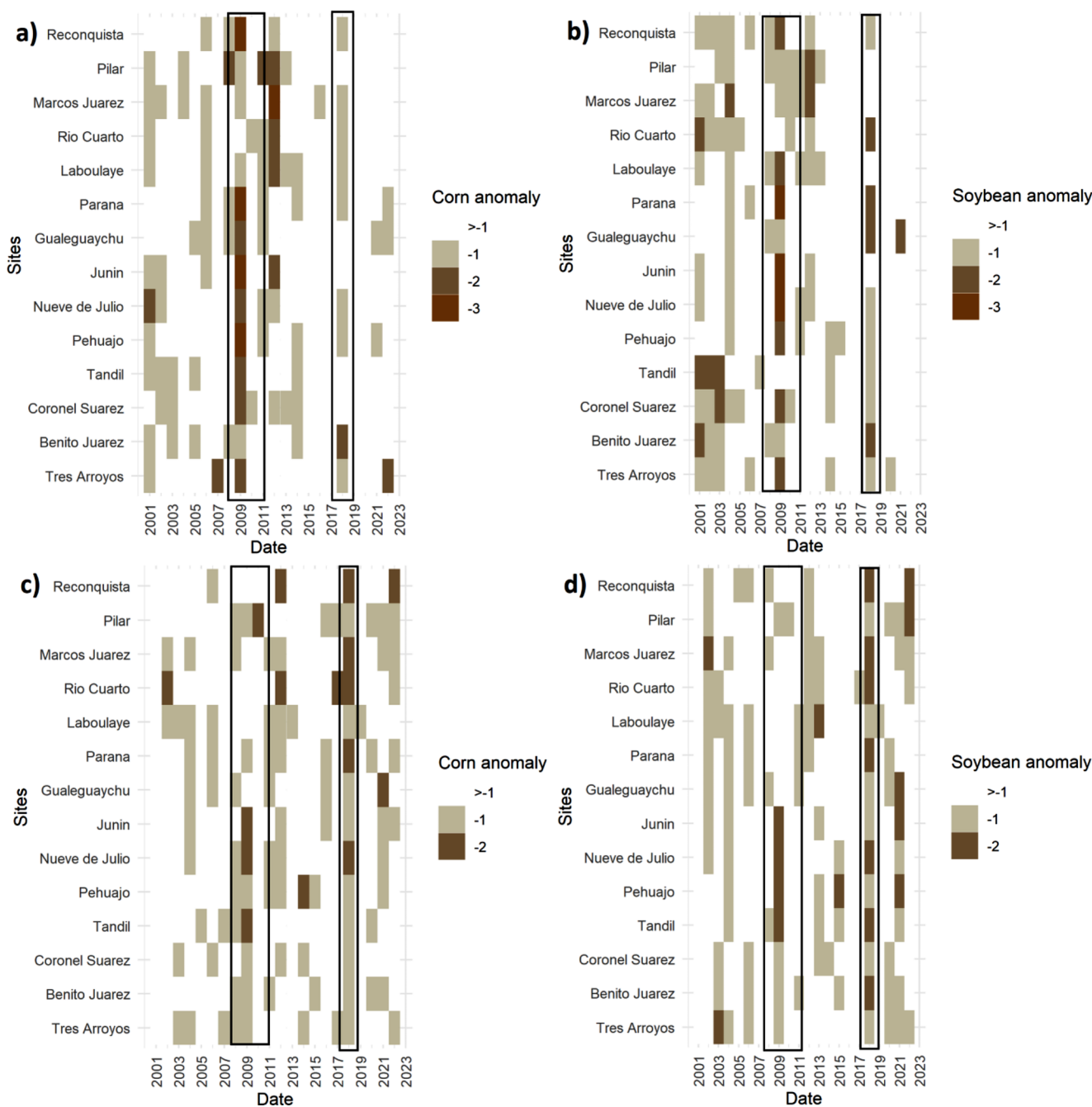


Fig. 4 Heatmap plots of corn and soybean yield standardized anomaly estimations (a) and (b) respectively) and corn and soybean standardized anomaly simulations (c) and (d) respectively) for the 14 locations

(ordered from north to south) over 2001–2022. The rectangles denote the 2008–2009 and 2017–2018 drought events

and Laboulaye) during 2011, 2012, and 2014. Notably, Pilar issued an agricultural emergency declaration for a portion of this period (2011–2012), further corroborating the CDI’s effective performance.

A reasonable agreement was observed between yield anomaly estimations and simulations. For instance, in Río Cuarto, both datasets indicated soybean negative anomalies less than -2 during the 2017–2018 event, while for corn,

there was concurrence, albeit with simulations showing greater deviations from the mean than yield estimations. Río Cuarto stands out due to having the highest median harvested area for both corn and soybean among the analyzed sites (refer to Table S2). In most cases, both the 2008–2009 and 2017–2018 events exhibit higher absolute negative anomalies in corn and soybean simulations compared to estimations. A comparison of ensemble crop simulations

and estimations for corn and soybean is provided for 3 locations (see Figure S1). In general, the yield simulations show a positive bias for both summer crops. However, during drought events, they both consistently depict lower yield values, exhibiting a median Spearman correlation of $r=0.57$ for soybeans and $r=0.52$ for corn across the 14 locations. When analyzing these correlation values, it must be taken into account that the median of the ensemble simulations was used for each location, along with the different spatial scales associated with each crop yield dataset.

In summary, there is an overall good consistent pattern observed between periods with a higher number of dekads in CDI's WARNING and ALERT categories, periods with agricultural emergency declarations, and the estimated and simulated yield anomalies of soybean and corn.

To quantitatively assess CDI performance, the relationship between the cumulative frequency of CDI drought categories (WATCH+WARNING+ALERT) and annual yield anomalies was evaluated using the ranked Tau correlations over the entire 2001–2022 period and for each site. The median of these correlations was then calculated for the 14 sites. To identify periods of high sensitivity, the correlation between CDI drought categories and crop yields were analyzed in 2 cases outlined in Table 2: (1) considering the entire crop growth cycle and (2) focusing only on the critical growth months for each crop. This analysis encompassed both yield estimations and ensemble simulations of corn and soybean anomalies.

A stronger negative correlation was observed, indicating a higher number of dekads under drought category associated with reduced yield values, when considering only the critical growth months for both crops against the CDI drought categories. This behavior is consistent for both soybean and corn yield estimations and simulations. Notably, during the critical period, the median correlation is higher for soybean ($r=-0.46$) compared to corn ($r=-0.40$) yield estimates. Conversely, for yield simulations, the same correlation value ($r=-0.50$) was obtained for both crops during the critical growth period. Additionally, it is important to highlight that median correlations are relatively stronger in simulations compared to estimations. Furthermore, the variability among sites based on the data range is more pronounced for both corn and soybean estimations and

simulation across the entire phenological cycle compared to the critical growth period.

Both 2008–2009 and 2017–2018 drought events that affected the Humid Pampas, exhibit remarkably different characteristics in severity, temporal evolution, and intensification rate, however, all had significant impact on agricultural yield. Therefore, the spatial and temporal evolution of these two events based on CDI were analyzed in the following sections.

3.1 2008–2009 drought event

The 2008–2009 drought persisted over a prolonged period, exhibiting a gradual onset, ranking among the most severe droughts with respect to spatial extension and severity between 1970 and 2010. It impacted nearly 50% of Argentina's population and nearly 30% of cropland, experiencing moderate drought conditions (Naumann et al. 2019). Initially linked to an intense La Niña event, which later persisted as a moderate La Niña event accompanied by inter-decadal, decadal and intraseasonal variability modes that collectively favored the lack of rainfall over the region (Fossa Riglos et al. *under review*).

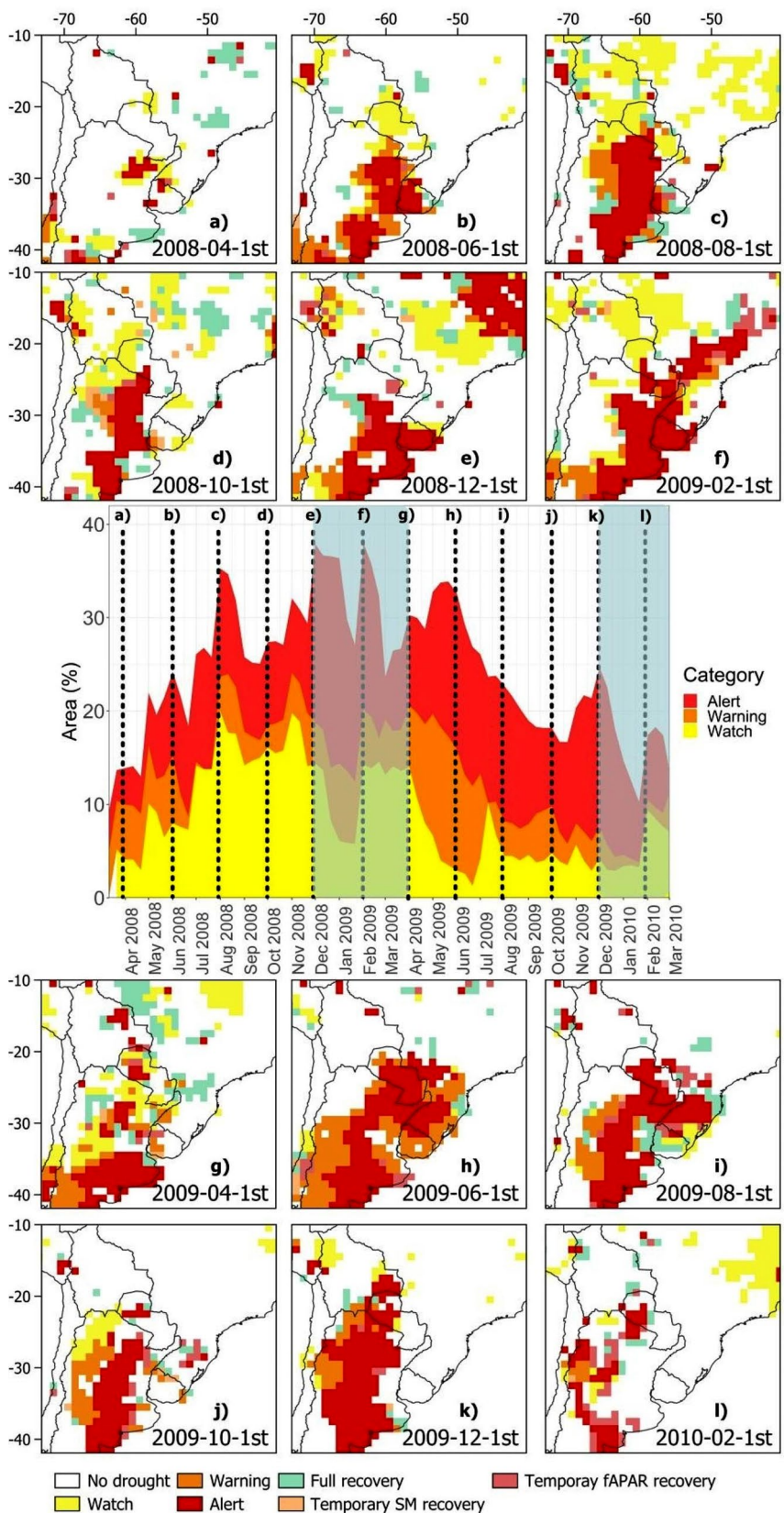
Figure 5 illustrates the temporal and spatial evolution of the event based on CDI. It can be observed how the event begins first in the north of the Argentine Humid Pampas (Fig. 5a), followed by a considerable spatial expansion in the next 2 and 4 months (Fig. 5b and c), encompassing 13%, 23%, and 36% of the area, respectively, based on the total number of pixels in the domain. In December 2008 (Fig. 5e) the maximum spatial extension under all 3 drought categories was observed, mainly linked to an increase in the grid cells in ALERT (22%) in the northeast of the domain, located in Brazil. By February 2009 (Fig. 5f), coinciding with the critical growth periods of corn and soybean, most of the Humid Pampas were affected by drought conditions, showing also a high spatial percentage for grid cells in ALERT drought category (17%).

Subsequent months continued to exhibit constant ALERT conditions for the region. Particularly noteworthy is the consistent high ALERT percentage (17%), once again observed during the critical growth period of summer crops in December 2009 (Fig. 5k). The drought severity, based on

Table 2 Median, maximum and minimum Tau correlations, over the 14 location sites, between corn and soybean yield estimations/simulations and the frequency/sum of dekads under CDI categories of WATCH, WARNING and ALERT. The complete crop campaign (September–March) and the critical growth periods for both summer crops were considered over the 2001–2022 period

Crop	Period	Yield estimations			Yield simulations		
		Median	Max	Min	Median	Max	Min
Corn	2001/02 to 2021/22	-0.30	-0.61	-0.06	-0.36	-0.61	-0.14
Corn	Dec to Feb	-0.40	-0.66	-0.13	-0.50	-0.55	-0.20
Soybean	2001/02 to 2021/22	-0.28	-0.49	-0.18	-0.29	-0.61	-0.05
Soybean	Dec to Mar	-0.46	-0.60	-0.29	-0.50	-0.60	-0.23

Fig. 5 CDI evolution during the 2008–2009 drought event. Panels show the CDI category evolution, with a time interval of 2 months. The central panel represents the % of pixels under each drought category based on the total amount of pixels of the domain. Shaded blue represents the critical growth period for corn and soybean together (December-February and December-March respectively)



the CDI, is consistent with the agricultural emergency declarations issued across all locations (refer to Fig. 3).

3.2 2017–drought event

In contrast to the 2008–2009 drought event, the 2017–2018 event developed as a flash drought (Kucheruck et al. 2024) across various sites in the Argentine Humid Pampas. This event was linked to a weak La Niña event and intraseasonal modes of atmospheric variability, leading to record lows in precipitation levels coupled with elevated temperatures, including heat waves, during early 2018 in the Humid Pampas (GAR, 2021).

In Fig. 6, the evolution of the CDI is shown, similarly to Fig. 5, but in this case with monthly intervals. Early evidence on the emergence of drought conditions can be observed in northern Argentina (Fig. 6a), with a rapid intensification of the drought conditions reaching the WARNING class in January 2018 (Fig. 6b). Concurrently, WATCH categories start appearing in the southern part of the Humid Pampas domain. By February 2018 (Fig. 6c), some WATCH areas escalate to WARNING conditions, with a worsening in terms of the surface area under WARNING (7%) conditions during March (Fig. 6d). The drought severity peaks in April and May 2018 (Fig. 6e and f), impacting vegetation over 10% of the total area according to CDI.

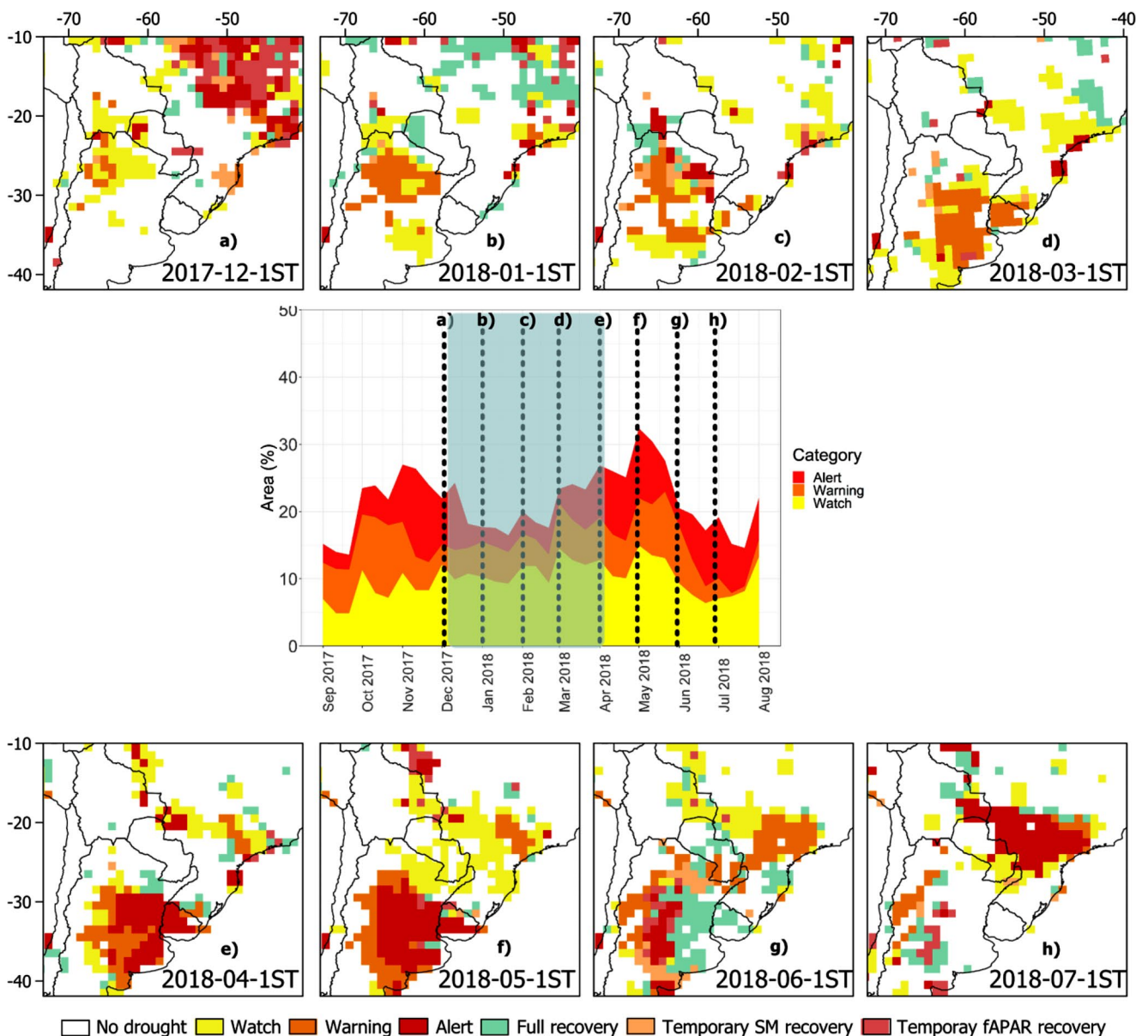


Fig. 6 CDI evolution during the 2017–2018 event. Panels show the CDI category evolution with a time interval of 1 month. The central panel represents the % of pixels under each drought category. Shaded

blue represents the critical growth period for corn and soybean together (December–February and December–March respectively)

In June 2018 signs of recovery can be observed, with a full cessation of drought conditions by July of the same year (Fig. 6g and h, respectively). It is important to note that while the percentage of area affected by drought categories was lower than in the 2008–2009 event, the 2017–2018 event predominantly affected the Argentine Humid Pampas, specifically during the latter part of the critical growth period of both analyzed crops. This intense, albeit relatively short, event highlights the importance of the timing of the drought, and the high impact that can be associated with events occurring during the critical growth periods of corn and soybean crops. This observation is consistent with the number of locations (9 of 14) that issued agricultural emergency declarations.

4 Discussion and conclusions

Based on the results of this study, encompassing both southern South America and 14 locations of the Argentine Humid Pampas, it can be confirmed that the correlations between SPI, soil moisture and fAPAR vary at different temporal lags. In general, within the Humid Pampas, the highest agreement was found at temporal lags ranging from 0 to 20 days (0 to +2d) between the precipitation deficit and soil moisture anomalies, lags of 0 to 20 days between soil moisture and fAPAR anomalies, and a lag of 10 to 30 days (+1d to +3d) between SPI and fAPAR anomalies. This finding further supports the need for a combined drought indicator that captures multiple observations of the various states and fluxes of the land-atmosphere boundary.

Notably, the correlation values across the 14 sites were slightly higher compared to those documented over Europe by Sepulcre-Canto et al. (2012) when comparing SPI-3, soil moisture and fAPAR anomalies. It is worth mentioning the higher correlation values between soil moisture and fAPAR observed over the Humid Pampas compared to Europe ($r=0.54$ vs. $|r|=0.35$). While this could be related to the difference in the analyzed period and/or to the region, it could also be due to a better representation of the ensemble soil moisture product currently used in the CDI. Given that the CDI evaluation performed by Sepulcre-Canto et al. (2012), used only the LISFLOOD soil moisture simulations. Furthermore, despite the different climatic regimes, the temporal lag of maximum correlation across the 14 sites aligns with those documented in Europe, highlighting similarities in temporal signals across variables over both agricultural regions.

The better agreement between SPI-3 and soil moisture and fAPAR anomalies compared to SPI-1, may be attributed to the longer accumulation period of SPI-3 as documented by Ji et al. (2003) over the Great Plains of the United States.

The authors performed an evaluation of different SPI accumulation periods against the Normalized Difference Vegetation Index (NDVI) and found that the highest correlation values were found for SPI-3 and NDVI, highlighting the lagged and cumulative effect of precipitation on vegetation. Furthermore, the authors noted that the correlation showed fluctuations among the growing season, peaking during the middle of the growing season. The latter feature could be related to the different crop critical growing periods, as it was also documented in this study for soybean and corn summer crops.

Other studies focused on the vegetation-soil moisture time response, like Ahmed et al. (2017), which analyzed the relationship between simulated soil moisture and NDVI over the Sahel region. The authors documented a strong NDVI-soil moisture relationship, with the highest correlation values for simultaneous and 1 month temporal lag, with a strong influence of the vegetation cover on the NDVI-soil moisture time response. For cropland and grassland, the authors observed a shorter time lag response (i.e. simultaneous and 1 month), while a longer time lag was observed for forest and deciduous shrubland. While the study of Ahmed et al. (2017) focused on a monthly time scale, similar lagged times responses spanning from 0 to 20 days were documented in this study between fAPAR and soil moisture over the Humid Pampas. In addition, Mladenova et al. (2019, 2020), quantified a similar lag correlation of satellite-based global soil moisture and NDVI, and demonstrated the utility of satellite-based soil moisture for assessing agricultural drought with lag correlation varying by climate zones and land cover type.

Over South America, Rossi et al. (2023), analyzed the drought propagation signal for different events focusing on meteorological aspects (i.e. precipitation deficit) leading to terrestrial water storage deficits over 3 different biomes in Brazil. In particular, the authors documented different timing responses between the precipitation deficit signal through soil moisture and vegetation, ranging from 1 up to 7 months across the biomes considered.

The findings of the studies mentioned above highlight the role of the different climates, vegetation cover and biomes on the temporal lagged relationships between the terrestrial hydrological variables. This aspect came forth in this study, when the lagged correlations for the whole domain were analyzed, showing regions with no significant correlation values and others with values above $r=0.60$. Across the Humid Pampas there is in general a ± 10 days time lag around the maximum correlation value between SPI, soil moisture and fAPAR anomalies which is not significantly different. This suggests potential flexibility of the CDI concerning near real time data availability, meaning that the utilization of different time lags may not significantly impact

the CDI outcomes. Although not the primary focus of this study, these results could serve as a starting point for analyzing temporal relationships between these variables to enhance drought onsets and recovery prediction.

The CDI accurately represented the onset, temporal and spatial evolution of both distinct 2008–2009 and 2017–2018 drought events. Based on the number of dekads under WARNING and ALERT categories, the CDI demonstrated consistency with periods when agricultural emergency declarations were issued, and with periods of negative soybean and corn yield estimations and simulations. Moreover, the indicator also showed a stronger correlation with agricultural impacts during the critical phenology growth periods compared to considering the whole crop season over the Humid Pampas. This outcome emphasizes that CDI severity more accurately captures the critical temporal stages when soybean and corn crops are most vulnerable to drought. Notably, this consistency persists despite the different spatial scales and uncertainties in estimations and simulations, thereby enhancing the robustness of CDI impact results.

Despite using a relatively coarse spatial resolution (i.e. $1^\circ \times 1^\circ$) and updating SPI on a monthly temporal frequency, the CDI proved to adequately represent the spatial and temporal propagation of the 2017–2018 flash drought event. However, in some locations (e.g. Marcos Juarez and Parana, Fig. 3) during this event, the CDI transitioned directly from no-drought category to WARNING, without the early warning WATCH category. This aspect could be improved if the SPI-1 and SPI-3 calculations are more frequently performed (e.g. every dekad), in order to better represent the temporal progression of the drought.

Conducting sensitivity tests on variables and drought indices by adjusting thresholds may improve the representation of the temporal propagation, and thus avoiding abrupt changes between categories (e.g. from no-drought to WARNING or ALERT). This may acquire high relevance when, for instance, a sequence of months that exhibits negative values of SPI between 0 and -1 (e.g. -0.6 , -0.9), affects a region but without triggering the WATCH category. The CDI could change under this hypothetical scenario from no-drought to WARNING or ALERT category as the precipitation accumulation deficit, if it persists through time, can negatively affect soil moisture and vegetation biomass/greenness. In addition to this, further potential enhancements for CDI should point to improving the spatial resolution for precipitation. A finer spatial resolution can be decisive for identifying drought-affected regions, like for example in departments with relatively small areas such as Coronel Suarez covering 5,985 km² (i.e. less than 1 pixel 10,000 km²). In this sense, a precipitation dataset like the Climate Hazards Group InfraRed Precipitation with

Station data (Funk et al. 2015) with a finer spatial resolution ($0.05^\circ \times 0.05^\circ$) could be an alternative to be tested.

The CDI is globally utilized for monitoring the risks associated with agricultural drought impact. Consequently, evaluating the construction and representation of drought severity in the CDI holds significant global and regional importance. Additionally, the effective utilization and prospective regional enhancements of the CDI play a crucial role in advancing drought monitoring and representation for the Humid Pampas, Argentina, and the CRC-SAS region. Achieving this goal requires fostering robust and seamless collaboration among all involved institutions. Subsequent research endeavors will strive to enhance the temporal and spatial capabilities of CDI, fortifying its role as a drought early warning system.

Supplementary Information The online version contains supplementary material available at <https://doi.org/10.1007/s00704-024-05073-8>.

Acknowledgements The data for this work were acquired through the Global Drought Observatory portal (<https://edo.jrc.ec.europa.eu/gdo>) and through the Secretaria de Agricultura, Ganadería y Pesca of Argentina.

Author contributions P.S., G.N. and C.C. wrote the main manuscript text. M.P. and P.S. prepared all figures. A.B. conducted the crop simulations. M.M. conducted bootstrap analysis. All authors reviewed the manuscript.

Data availability No datasets were generated or analysed during the current study.

Declarations

Competing interests The authors declare no competing interests.

References

- Ahmed M, Else B, Eklundh L, Ardö J, Seaquist J (2017) Dynamic response of NDVI to soil moisture variations during different hydrological regimes in the Sahel. *Int J Remote Sens* 38(19):5408–5429. <https://doi.org/10.1080/01431161.2017.1339920>
- Aramburu Merlos F, Monzon JP, Mercau JL et al (2015) Potential for crop production increase in Argentina through closure of existing yield gaps. *Field Crops Res* 184:145–154. <https://doi.org/10.1016/j.fcr.2015.10.001>
- Cammalleri C, Vogt JV, Bisselink B, de Roo A (2017) Comparing soil moisture anomalies from multiple independent sources over different regions across the globe. *Hydrol Earth Syst Sci* 21:6329–6343. <https://doi.org/10.5194/hess-21-6329-2017>
- Cammalleri C, Arias-Muñoz C, Barbosa P et al (2021) A revision of the Combined Drought Indicator (CDI) used in the European Drought Observatory (EDO). *Nat Hazards Earth Syst Sci* 21:481–495. <https://doi.org/10.5194/nhess-21-481-2021>
- De Roo A, Wesseling C, Van Deursen W (2000) Physically based river basin modeling within a GIS: the

- LISFLOOD model. *Hydrol Process* 14:1981–1992. [https://doi.org/10.1002/1099-1085\(20000815/30\)14:11/12%3C1981::AID-HYP49%3E3.0.CO;2-F](https://doi.org/10.1002/1099-1085(20000815/30)14:11/12%3C1981::AID-HYP49%3E3.0.CO;2-F)
- Donatti CI, Nicholas K, Fedele G, Delforge D, Speybroeck N, Moraga P, Blatter J, Below R, Zvoleff A (2024) Global hotspots of climate-related disasters. *Int J Disaster Risk Reduct* 108:2212–4209. <https://doi.org/10.1016/j.ijdrr.2024.104488>
- Dorigo WA, Wagner W, Albergel C et al (2017) ESA CCI Soil Moisture for improved Earth system understanding: state-of-the art and future directions. *Remote Sens Environ*. <https://doi.org/10.1016/j.rse.2017.07.001>
- Funk C, Peterson P, Landsfeld M et al (2015) The climate hazards infrared precipitation with stations—a new environmental record for monitoring extremes. *Sci Data* 2:150066. <https://doi.org/10.1038/sdata.2015.66>
- Gobron N, Pinty B, Mélin F et al (2005) The state of vegetation in Europe following the 2003 drought. *Int J Remote Sens* 26(9):2013–2020. <https://doi.org/10.1080/01431160412331330293>
- Gruber A, Su C-H, Zwieback S, Crow W, Dorigo W, Wagner W (2016) Recent advances in (soil moisture) triple collocation analysis. *Int J Appl Earth Observation Geoinf* 45(Part B 200–211). <https://doi.org/10.1016/j.jag.2015.09.002>
- Gruber A, Scanlon T, van der Schalie R, Wagner W, Dorigo W (2019) Evolution of the ESA CCI soil moisture climate data records and their underlying merging methodology. *Earth Syst Sci Data* 11:717–739. <https://doi.org/10.5194/essd-11-717-2019>
- Hendrawan VSA, Kim W, Touge Y, Ke S, Komori D (2022) A global-scale relationship between crop yield anomaly and multiscalar drought index based on multiple precipitation data. *Environmental Research Letters*, 17(1), p.014037
- Hoogenboom G, Jones JW, Wilkens PW et al (2010) Decision support system for Agrotechnology transfer (DSSAT) Version 4.5. [CD-ROM]. Univ. of Hawaii, Honolulu
- Ji L, Peters AJ (2003) Assessing vegetation response to drought in the northern Great Plains using vegetation and drought indices, *Remote Sensing of Environment*, Volume 87, Issue 1, Pages 85–98, ISSN 0034-4257, [https://doi.org/10.1016/S0034-4257\(03\)00174-3](https://doi.org/10.1016/S0034-4257(03)00174-3)
- Kim W, Iizumi T, Nishimori M (2019) Global patterns of crop production losses associated with droughts from 1983 to 2009. *J Appl Meteorol Climatol* 58(6):1233–1244
- Kim H, Crow WT, Wagner W, Li X, Lakshmi V (2023) A bayesian machine learning method to explain the error characteristics of global-scale soil moisture products. *Remote Sens Environ* 296:113718
- Kucheruk L, Spennemann PC, Naumann G, Rivera JA (2024) Climatología de Sequías de Rápido Desarrollo en la Pampa Húmeda Argentina. *Meteorológica*, Vol. 49, e025, ISSN 1850-468X <https://doi.org/10.24215/1850468Xe025> Centro Argentino de Meteorólogos Buenos Aires – Argentina
- McKee TB, Doesken NJ, Kleist J (1993) The relationship of drought frequency and duration of time scales. Eighth Conference on Applied Climatology, American Meteorological Society, Jan17–23, 1993, Anaheim CA, pp.179–186
- Mercau JL, Dardanelli JL, Collino DJ, Andriani JM, Irigoyen A, Satorre EH (2007) Predicting on-farm soybean yields in the pampas using CROPGRO-soybean. *Field Crops Res* 100(2–3):200–209
- Mladenova IE, Bolten JD, Crow WT, Sazib N, Cosh MH, Tucker CJ, Reynolds C (2019) Evaluating the operational application of SMAP for Global Agricultural Drought Monitoring. *IEEE J Sel Top Appl Earth Observations Remote Sens* 1–11. <https://doi.org/10.1109/jstars.2019.2923555>
- Mladenova IE, Bolten JD, Crow W, Sazib N, Reynolds C (2020) Agricultural Drought Monitoring via the assimilation of SMAP Soil Moisture retrievals into a global Soil Water Balance Model. *Front Big Data*. 3<https://doi.org/10.3389/fdata.2020.00010>
- Monzon JP, Sadras VO, Andrade FH (2012) Modelled yield and water use efficiency of maize in response to crop management and Southern Oscillation Index in a soil-climate transect in Argentina. *Field Crops Res* 130:8–18
- Naumann G, Vargas WM, Barbosa P, Blauhut V, Spinoni J, Vogt JV (2019) Dynamics of socioeconomic exposure, vulnerability and impacts of recent droughts in Argentina. *Geosciences* 9:39
- Naumann G, Podesta G, Marengo J et al (2021) The 2019–2021 extreme drought episode in La Plata Basin. EUR 30833 EN. Publications Office of the European Union, Luxembourg. <https://doi.org/10.2760/346183>
- Naumann G, Podesta G, Marengo J et al (2023) Extreme and long-term drought in the La Plata Basin: event evolution and impact assessment until September 2022. EUR 31381 EN, Publications Office of the European Union, Luxembourg. <https://doi.org/10.2760/62557>
- Otkin JA, Svoboda M, Hunt ED, Ford TW, Anderson MC, Hain C, Basara JB (2018) Flash droughts: a Review and Assessment of the challenges imposed by Rapid-Onset Droughts in the United States. *Bull Amer Meteor Soc* 99:911–919. <https://doi.org/10.1175/BAMS-D-17-0149.1>
- Peng J, Muller JP, Blessing S et al (2019) Can we use Satellite-based FAPAR to Detect Drought? *Sensors* 19(17):3662. <https://doi.org/10.3390/s19173662>
- Rossi JB, Ruhoff A, Fleischmann AS, Laipelt L (2023) Drought Propagation in Brazilian biomes revealed by Remote Sensing. *Remote Sens* 15:454. <https://doi.org/10.3390/rs15020454>
- SAGyP (2022) Ministerio de Agricultura, Ganadería y Pesca, Oficina de Monitoreo de Emergencias y Desastres Agropecuarios. Acceso Mayo, 2022. [Online]. https://www.agroindustria.gob.ar/sitio/areas/d_eda/resoluciones/
- Sánchez N, González-Zamora Á, Piles M, Martínez-Fernández JA (2016) A New Soil Moisture Agricultural Drought Index (SMADI) integrating MODIS and SMOS products: a case of study over the Iberian Peninsula. *Remote Sens* 8:287. <https://doi.org/10.3390/rs8040287>
- Schamm K, Ziese M, Becker A et al (2014) Global gridded precipitation over land: a description of the new GPCC First guess daily product. <https://doi.org/10.5194/essd-6-49-2014>. *Earth System Science Data*
- Sepulcre-Canto G, Horion S, Singleton A, Carrao H, Vogt J (2012) Development of a Combined Drought Indicator to detect agricultural drought in Europe. *Nat Hazards Earth Syst Sci* 12:3519–3531. <https://doi.org/10.5194/nhess-12-3519-2012>
- Spennemann PC, Rivera JA, Saulo AC, Penalba OC (2015) A comparison of GLDAS soil moisture anomalies against standardized precipitation index and multisatellite estimations over South America. *J Hydrometeorology* 16:158–171. <https://doi.org/10.1175/JHM-D-13-0190.1>
- Spennemann PC, Fernández-Long ME, Gattinoni NN, Cammalleri C, Naumann G (2020) Soil moisture evaluation over the Argentine Pampas using models, satellite estimations and in-situ measurements. *J Hydrology: Reg Stud* 31:100723. <https://doi.org/10.1016/j.ejrh.2020.100723>
- Spinoni J, Barbosa P, Bucchignani E et al (2020) Future Global Meteorological Drought Hot spots: a study based on CORDEX Data. *J Clim* 33(9):3635–3661. <https://doi.org/10.1175/JCLI-D-19-0084.1>
- Svoboda M, LeComte D, Hayes M et al (2002) THE DROUGHT MONITOR. *Bull Am Meteorol Soc* 83(8):1181–1190. <https://doi.org/10.1175/1520-0477-83.8.1181>
- Thi NQ, Govind A, Le MH, Linh NT, Anh TTM, Hai NK (2023) Spatio-temporal characterization of droughts and vegetation response in

- Northwest Africa from 1981 to 2020. *Egypt J Remote Sens Space Sci* 26(3):393–401. <https://doi.org/10.1016/j.ejrs.2023.05.006>
- Thomasz EO, Vilker AS, Rondinone G (2019) The economic cost of extreme and severe droughts in soybean production in Argentina. *Contaduría Y Administración* 64(1):1–24. <https://doi.org/10.22201/fca.24488410e.2018.1422>
- United Nations Office for Disaster Risk Reduction (2021) Global Assessment Report (GAR): Special Report on Drought. 9789212320274
- Vicente-Serrano SM, Beguería S, López-Moreno JI (2010) A Multiscale Drought Index sensitive to global warming: the standardized precipitation Evapotranspiration Index. *J Clim* 23:1696–1718. <https://doi.org/10.1175/2009JCLI2909.1>
- Wan Z, Zhang Y, Zhang Q, Li ZL (2002) Validation of the land surface temperature products retrieved from Terra Moderate Resolution Imaging Spectroradiometer data. *Remote Sens Environ* 83:163–180
- World Meteorological Organization (WMO) and Global Water Partnership (GWP) (2016) Handbook of Drought Indicators and Indices (Svoboda M and Fuchs BA), Integrated Drought Management Programme (IDMP), Integrated Drought Management Tools and Guidelines, Series 2, Geneva, Switzerland, 45, <https://public.wmo.int/en/resources/library/standardized-precipitation-index-user-guide2016>

Publisher's Note Springer Nature remains neutral with regard to jurisdictional claims in published maps and institutional affiliations.

Springer Nature or its licensor (e.g. a society or other partner) holds exclusive rights to this article under a publishing agreement with the author(s) or other rightsholder(s); author self-archiving of the accepted manuscript version of this article is solely governed by the terms of such publishing agreement and applicable law.